Division of Engineering
BROWN UNIVERSITY
PROVIDENCE, R. I.

# THE EFFECT OF AN ELASTIC MEMBRANE ON THE STABILITY OF A TRIAXIAL TEST OF A TIME INDEPENDENT SOIL

J. B. WEIDLER and P. R. PASLAY



Department of Defense
Advanced Research Projects Agency
Contract SD-86
Materials Research Program

ARPA E47

July 1967

# THE EFFECT OF AN ELASTIC MEMBRANE ON THE STABILITY OF A TRIAXIAL TEST OF A TIME INDEPENDENT SOIL

by

Jay B. Weidler and Paul R. Paslay

Division of Engineering
Brown University
Providence, Rhode Island

July, 1967

# THE EFFECT OF AN ELASTIC MEMBRANE ON THE STABILITY OF A TRIAXIAL TEST OF A TIME INDEPENDENT SOIL*

by

Jay B. Weidler** and Paul R. Paslay***

Using an analytical model to represent the soil and an elastic-membrane theory to represent the sheath commonly used around the soil sample the stability of the soil-membrane system is studied. The measure of stability used is the time derivative of the rate of doing work by the external loading for a prescribed motion.

The results give a means of evaluating the relative effect of the membrane on the initial stability of the ststem. A numerical example shows the effect to be negligible in the case of the initial stability of a particular soil.

---

* The research reported here was supported by ARPA Contract E-47.

** Assistant Professor of Engineering(Research), Brown University.

*** Professor of Engineering, Brown University.

## Introduction

In an earlier work [1]* the authors have attempted to generalize the usual approach to time independent continuum soil mechanics. It has been popular recently, for example see [2], to use a perfectly plastic Coulomb-Mohr theory with an associated flow rule determined from the normality of the incremental plastic strain vector to the yield surface. The theory proposed by the authors differs from such an approach in the following respects

a. The loading surface, instead of diverging with increasing hydrostatic pressure, closes and is intersected by the spherical stress axis at specific value of hydrostatic pressure. Thus the loading surface is a closed surface.

b. The size of the loading surface varies for each point according to the value of the specific volume at that point.

c. The normality of the incremental strain vector to the loading surface at each point is replaced by a set of permissible directions which happen to always include normality. The permissible directions are deduced from energy considerations that include an internal energy U which depends on the specific volume.

---

* Numbers in brackets designate references listed in the bibliography.

Using a specific case of the above theory the deformations occuring in a triaxial test (a compression test in the presence of hydrostatic pressure) were studied [3] by the authors. This work neglected the presence of a membrane around the cylindrical sample. In this study of the triaxial test two possible deformation modes were considered. The first was a homogeneous deformation of the entire sample, shown in Figure 1a, while the second was a shearing motion of an inclined layer of the material, depicted in Figure 1b. The results of sample calculations were given for an analytical model whose properties were similar to a uniform Leighton Buzzard sand which has been reported in [4]. For the model the homogeneous deformation indicated an initially positive value for the time rate of change of the rate at which the external loads do work on the soil sample. For the same quantity, which will be denoted by $\ddot{W}$, the shearing motion indicated an initially negative value. A positive value of $\ddot{W}$ indicates a stable system while an unstable system is predicted by a negative value of $\ddot{W}$. The actual magnitudes of $\ddot{W}$ serve also as measures of the stability or instability of the system. Consequently of all possible modes of motion, the mode with the lowest measure of stability, $\ddot{W}$, is hypothesized as the one which in actuality will occur. For the shearing motion, $\ddot{W}$ was also shown in [3] to be inversely proportional to the thickness H of the shearing layer as shown in Figure 1b. For the numerical example where $\ddot{W}$ was shown to have a negative sign, the value of H producing the largest negative $\ddot{W}$ is H equal to zero leading to $\ddot{W}$ equal to minus infinity. Therefore for the modes considered a displacement discontinuity across an inclined plane, as depicted in Figure 2, is the anticipated actual mode of deformation.

In connection with the shearing mode of deformation a change in loading procedure develops which is not present in the homogeneous deformation. The

The initial state of loading is a uniform hydrostatic, $-\sigma_L$, and a superimposed compressive stress, $-\sigma_C$, for all modes of deformation. In order to induce the shearing mode a non-trivial rate of change of shearing stress $\sigma_{yz}$, see Figure 2, must be present. It is assumed in the following that this loading is supplied by the testing device while the sample undergoes the initiation of shearing motion.

It is the purpose of the current work to present an evaluation of the effect of a membrane surrounding the sample in the case of the shearing motion in the triaxial test. The impermeable membrane is generally employed to help maintain the integrity of the soil sample before loading commences and to sustain the hydrostatic loading applied to the sample. That is, in the triaxial test there is a pore pressure in the sample which is maintained under prescribed conditions (in this work the pore pressure is always zero) while the external hydrostatic pressure is applied to the sample independent of the pore pressure. In the current considerations both the pore pressure and the external hydrostatic pressures are held constant so that

$$\text{hydrostatic pressure} - \text{pore pressure} = -\sigma_L \qquad (1)$$

throughout the test.

## Time Independent Soil Under Consideration

The description of the soil under consideration is reviewed in this section. More detail concerning this description may be found in [3]. The functions used are as follows:

$v$ = specific volume, volume per unit weight of soil sample.

$\phi = \phi(v)$ = friction angle for Coulomb-Mohr part of loading surface.

$c = c(v)$ = cohesive strength for Coulomb-Mohr part of yield surface.

$\sigma_o = \sigma_o(v)$ = mean normal stress associated with the closing of the yield surface on the compression side.

$U = U(v)$ = internal energy per unit weight of the soil sample.

$\sigma = 1/3\ (\sigma_x + \sigma_y + \sigma_z)$ = mean normal stress

$G = G(v,\sigma)$ = function which determines the direction for the incremental strain. When G is zero the vector is normal to the loading surface. When G equals $2 \sin\phi/[3\ (1 + \sin\phi)]$ the flow is incompressible. From [3], $0 \leq G = \alpha\ (\partial U/\partial v)\ (2 \sin\phi)\ /\ (3\ \{1 + \sin\phi\} \cdot \{\sigma_o - \sigma + \alpha\ [\partial U/\partial v]\}) \leq (2 \sin\phi)/(3[1 + \sin\phi])$ and $\alpha$ is a constant for this case.

Z, R, H = dimensions shown in Figure 1b.

$\dot{Z}$ = constant vertical velocity of compression loading device, Figure 2.

$\dot{Y}$ = lateral velocity of section of sample above shearing plane, Figure 2.

The following conditions are assumed satisfied in this investigation.

$$c(v) \geq 0 \tag{2.a}$$

$$0 \leq \phi\ (v) < \pi/2 \tag{2.b}$$

$$\frac{\partial \phi}{\partial v} \leq 0 \tag{2.c}$$

$$\sigma_o < \frac{\partial U}{\partial v} \leq 0 \tag{2.d}$$

$$\sigma > \sigma_o \tag{2.e}$$

$$0 < \alpha < 1 \tag{2.f}$$

$$1 > \kappa > 0 \tag{2.g}$$

In [3] it is shown that

$$\ddot{W}_{soil} = \pi\ R^2 Z\ (\dot{Z}\ /\ Z)^2\ S^{**} \tag{3}$$

where

$$S^{**} = (Z/H)\left[\dot{\sigma}_C/(\dot{Z}/H) + \{\dot{\sigma}_{yz}/(\dot{Z}/H)\}\{(\dot{Y}/H)/(\dot{Z}/H)\}\right] \tag{4}$$

and

$$\sigma_C = -2(c - \sigma_L)\frac{\sin\phi}{1 - \sin\phi} \tag{5.a}$$

$$\sigma = \sigma_C/3 + \sigma_L \tag{5.b}$$

$$\psi = (1/2)\cos^{-1}\left\{\frac{-2\sin\phi + 3G(1 + \sin\phi)}{2 - G(1 + \sin\phi)}\right\} \tag{5.c}$$

$$\dot{v}/(\dot{Z}/H) = \frac{v.\cos 2\psi}{\cos\psi} \tag{5.d}$$

$$(\dot{Y}/H)/(\dot{Z}/H) = -\tan\psi \tag{5.e}$$

$$\dot{\sigma}_C/(\dot{Z}/H) = -2\left[\frac{\sin\phi}{1-\sin\phi}\cdot\frac{\partial c}{\partial v} + (c-\sigma_L)\cdot\frac{\cos\phi}{(1-\sin\phi)^2}\frac{\partial\phi}{\partial v}\right]\cdot[\dot{v}/(\dot{Z}/H)] \tag{5.f}$$

$$\dot{\sigma}_{yz}/(\dot{Z}/H) = (\sigma_C/2\sin 2\psi)\left[\cos\phi\cdot\frac{(3G - 2 + G\cos 2\psi)}{2 - G(1 + \sin\phi)}\frac{\partial\phi}{\partial v}(\dot{v}/[\dot{Z}/H])\right.$$

$$\left. + \frac{(1 + \sin\phi)(3 + \cos 2\psi)}{2 - G(1 + \sin\phi)}\left\{\frac{\partial G}{\partial v}(\dot{v}/[\dot{Z}/H]) + \frac{1}{3}\frac{\partial G}{\partial\sigma}(\dot{\sigma}_C/[\dot{Z}/H])\right\}\right] \tag{5.g}$$

Consequently when the functions $\phi(v)$, $c(v)$, $\sigma_o(v)$, $U(v)$, and $G(v,\sigma)$ are known for the material then specification of v and $\sigma_L$ combined with the above equations determines $(H/Z)\ S^{**}$.

In [3] the following functions were used for the sample calculation where v is in cubic inches per pound:

$$\phi(v) = 0.686 - 0.100\ (v - 16.08)\quad \{\text{radians}\} \tag{6.a}$$

$$c(v) = 0 \tag{6.b}$$

$$\sigma_o(v) = -129\left(\frac{19.00 - v}{v - 16.08}\right)\quad \{\text{lbs/in}^2\} \tag{6.c}$$

$$\alpha U(v) = +12.9[-(19.00 - v) + 2.92\ \ln\{2.92/(v-16.08)\}]\ \{\text{inches}\} \tag{6.d}$$

$$G(v,\sigma) = \alpha\frac{\partial U}{\partial v}\cdot\frac{2\sin\phi}{3(1 + \sin\phi)(\sigma_o - \sigma + \alpha\frac{\partial U}{\partial v})} \tag{6.e}$$

with the following conditions

$$v = 16.83 \text{ in}^3/\text{lb} \tag{7.a}$$

$$\sigma_L = -50 \text{ lbs/in}^2 \tag{7.b}$$

These functions and conditions led to the following results for the shearing mode of deformation

$$(\frac{H}{Z})\ S^{**} = -1023 \tag{8.a}$$

$$\phi = 34.7^{\circ} \tag{8.b}$$

$$\sigma_o = -343 \text{ lbs/in}^2 \tag{8.c}$$

$$\sigma_C = -132 \text{ lbs/in}^2 \tag{8.d}$$

$$\sigma = -94 \text{ lbs/in}^2 \tag{8.e}$$

$$\psi = 60.4^{\circ} \tag{8.f}$$

$$\dot{v}/(\dot{Z}/H) = -17.48 \text{ in}^3/\text{lb} \tag{8.g}$$

$$(\dot{Y}/H)/(\dot{Z}/H) = -1.755 \tag{9.h}$$

$$\dot{\sigma}_C/\ (\dot{Z}/H) = -774 \text{ lbs/in}^2 \tag{8.i}$$

$$\dot{\sigma}_{yz}/(\dot{Z}/H) = +\ 142 \text{ lbs/in}^2 \tag{8.j}$$

Inclusion of Membrane Forces

In this analysis the membrane is treated as a thin walled elastic cylinder. For simplicity in describing the membrane behavior consider the single plane element shown in Figure 3. If the bending stiffness of this element is neglected then the deformation elements $\delta_\varepsilon$, $\delta_\gamma$, and $\delta b$ shown in Figure 3a induce the following forces shown in Figure 3b.

$$N = \delta_\varepsilon\ S\ H\ \bar{E}/\tilde{H} \tag{9.a}$$

$$T = \delta_\gamma\ S\ h\ \bar{G}/\tilde{H} \tag{9.b}$$

where h is the membrane thickness, $\bar{E}$ is the membrane Young's modulus and $\bar{G}$ is the membrane shear modulus.

The motion depicted in Figure 1b may be expressed in terms of $\dot{Y}$ and $\dot{Z}$. The displacement rate of the upper section of the cylinder denoted by $\dot{\vec{\delta}}$ is

$$\dot{\vec{\delta}} = (0)\,\vec{i} + (\dot{Y})\,\vec{j} + (\dot{Z})\,\vec{k} \tag{10}$$

It is useful to define a set of orthogonal unit vectors $\vec{n}$, $\vec{t}$, and $\vec{e}$ as shown in Figure 4. Set

$$\vec{n} = (\cos\theta)\,\vec{i} + (\sin\theta)\,\vec{j} + (0)\,\vec{k} \tag{11.a}$$

$$\vec{t} = [\cos^2\psi + \sin^2\psi\cos^2\theta]^{-1/2}\ [(-\sin\theta\cos\psi)\,\vec{i} + (\cos\theta\cos\psi)\,\vec{j} + (-\cos\theta\sin\psi)\,\vec{k}\,] \tag{11.b}$$

$$\vec{e} = [\cos^2\psi + \sin^2\psi\,\cos^2\theta]^{-1/2}\ [(-\sin\theta\cos\theta\sin\psi)\,\vec{i} + (\cos^2\theta\sin\psi)\,\vec{j} + (\cos\psi)\,\vec{k}\,] \tag{11.c}$$

At the instant flow begins the deformation rate components $\dot{\delta}_\varepsilon$ and $\dot{\delta}_\gamma$ may be defined as the projections of $\dot{\vec{\delta}}$ onto the $\vec{e}$ and $\vec{t}$ unit vectors respectively. Hence

$$\dot{\delta}_\varepsilon = \dot{\vec{\delta}}\cdot\vec{e} = [\cos^2\psi + \sin^2\psi\cos^2\theta]^{-1/2}\cdot[\dot{Y}\cos^2\theta\sin\psi + \dot{Z}\cos\psi] \tag{12.a}$$

$$\dot{\delta}_\gamma = \dot{\vec{\delta}}\cdot\vec{t} = [\cos^2\psi + \sin^2\psi\cos^2\theta]^{-1/2}\cdot[\dot{Y}\cos\theta\cos\psi - \dot{Z}\cos\theta\sin\psi] \tag{12.b}$$

Introducing a unit vector normal to the plane of shear

$$\vec{p} = (0)\,\vec{i} + (\sin\psi)\,\vec{j} + (\cos\psi)\,\vec{k} \tag{13}$$

a relationship between $\tilde{H}$ in Equations (9) and the thickness of the shearing layer, H, may be determined

$$H = \tilde{H}\,\vec{e}\cdot\vec{p} = \tilde{H}\,(\sin^2\psi\cos^2\theta + \cos^2\psi)^{1/2} \tag{14}$$

Using Equations (9) and (14), $\dot{\delta}_\varepsilon$ and $\dot{\delta}$ may also be defined as

$$\dot{\delta}_\varepsilon = \left(\frac{d\dot{N}}{dS}\right) \frac{H}{h\bar{E}} \cdot(\cos^2\theta\sin^2\psi + \cos^2\psi)^{-1/2} \tag{15.a}$$

$$\dot{\delta}_\gamma = \left(\frac{d\dot{T}}{dS}\right) \frac{H}{h\bar{G}} \cdot(\cos^2\theta\sin^2\psi + \cos^2\psi)^{-1/2} \tag{15.b}$$

The increment of length along the ellipse formed by the intersection of the shearing plane and the cylinder may be expressed in terms of $\theta$ by

$$dS = \frac{R(\cos^2\theta\sin^2\psi + \cos^2\psi)^{1/2}}{\cos\psi} \cdot d\theta \tag{16}$$

The rate of change of the force required to deform the membrane is denoted by $\dot{\vec{F}}$ and is defined by

$$\dot{\vec{F}} = \int_{\theta=0}^{\theta=2\pi} \left[\left(\frac{d\dot{N}}{dS}\right) \vec{e} + \left(\frac{d\dot{T}}{dS}\right) \vec{t}\ \right] dS \tag{17}$$

Making use of Equations (11), (12), (15) and (16), Equation (17) may be evaluated to yield

$$\dot{\vec{F}} = \frac{Rh\,\pi}{H\cos\psi} \left[\{0\}\vec{I} + \{(3/4)\,\bar{E}\sin^2\psi + \bar{G}\cos^2\psi)\,\dot{Y} + (\bar{E} - \bar{G})(\cos\psi\sin\psi)\dot{Z}\}\vec{j}\right.$$
$$\left. + \{(\bar{E} - \bar{G})(\cos\psi\sin\psi)\dot{Y} + (2\bar{E}\cos^2\psi + \bar{G}\sin^2\psi)\dot{Z}\}\vec{k}\right] \tag{18}$$

Using Equations (10) and (18), the time rate of change of the rate at which the external loads do work on the membrane may be evaluted. Denoting this quantity as $\ddot{W}_{\text{membrane}}$ it can be shown that

$$\ddot{W}_{\text{membrane}} = \dot{\vec{F}} \cdot \vec{\delta}$$
$$= \pi R^2 Z(\dot{Z}/Z)^2(Z/H)\cdot(h/R)\left[(\dot{Y}/\dot{Z})^2\,\frac{3\bar{E}\sin^2\psi + 4\,\bar{G}\cos^2\psi}{4\cos\psi} +\right.$$
$$\left. 2\,(\dot{Y}/\dot{Z})\,(\bar{E} - \bar{G})\sin\psi + \frac{2\bar{E}\cos^2\psi + \bar{G}\sin^2\psi}{\cos\psi}\right] \tag{19}$$

The quantity measuring the stability of the soil-membrane system is simply the sum of $\ddot{W}_{soil}$ and $\ddot{W}_{membrane}$. Thus

$$\ddot{W} = \ddot{W}_{soil} + \ddot{W}_{membrane}$$

$$= \pi R^2 Z (\dot{Z}/Z)^2 \left[S^{**} + (Z/H)(h/R) \left\{(\dot{Y}/\dot{Z})^2 \cdot \frac{3\bar{E}\sin^2\psi + 4\bar{G}\cos^2\psi}{4\cos\psi} + 2(\dot{Y}/\dot{Z})(\bar{E} - \bar{G})\sin\psi + \frac{2\bar{E}\cos^2\psi + \bar{G}\sin^2\psi}{\cos\psi}\right\}\right] \quad (20)$$

Using the numerical results of the example cited in the previous section with

$$\bar{E} = 200 \text{ psi} \quad (21.a)$$

$$\bar{G} = 66.7 \text{ psi} \quad (21.b)$$

yields

$$\ddot{W} = \pi R^2 Z(\dot{Z}/Z)^2 (Z/H)(-1023 + 702 \frac{h}{R}) \quad (22)$$

For cases of practical significance a typical value of h/R is 0.014. Clearly any h/R of interest is too small to make the sign of (-1023 + 702 h/R) positive and thus stabilize the system. The result is that any typical membrane has a very small stabilizing effect on the initial stability of a triaxial test for the material and initial state considered.

## Bibliography

1. J. B. Weidler and P. R. Paslay, "An Analytical Description of the Behavior of Granular Media," to be submitted for publication.

2. R. T. Shield, "On Coulomb's Law of Failure in Soils," Journal of the Mechanics and Physics of Solids, 1955, vol. 4, pp.10-16.

3. P. R. Paslay and J. B. Weidler, "An Analysis of the Triaxial Test for Cohesionless Soils," to be submitted for publication.

4. K. H. Roscoe, A. N. Schofield and A. Thurairajah, "An Evaluation of Test Data for Selecting a Yield Criterion for Soils," ASTM STP 361, Laboratory Shear Testing of Soils, 1964, pp. 111-128.

nfh

## FIGURE CAPTIONS

Figure 1 - Two Modes of Deformation for the Triaxial Test:

a) Homogeneous Deformation

b) Shearing Motion

Figure 2 - Mode of Deformation for Shearing Motion When the Corresponding $\ddot{W}$ is less than zero.

Figure 3 - Plane Element of Membrane Showing

a) Displacements

b) Forces

Figure 4 - Section of Thin Membrane Below Shearing Plane Showing Vectors $\vec{b}$, $\vec{c}$, and $\vec{e}$.

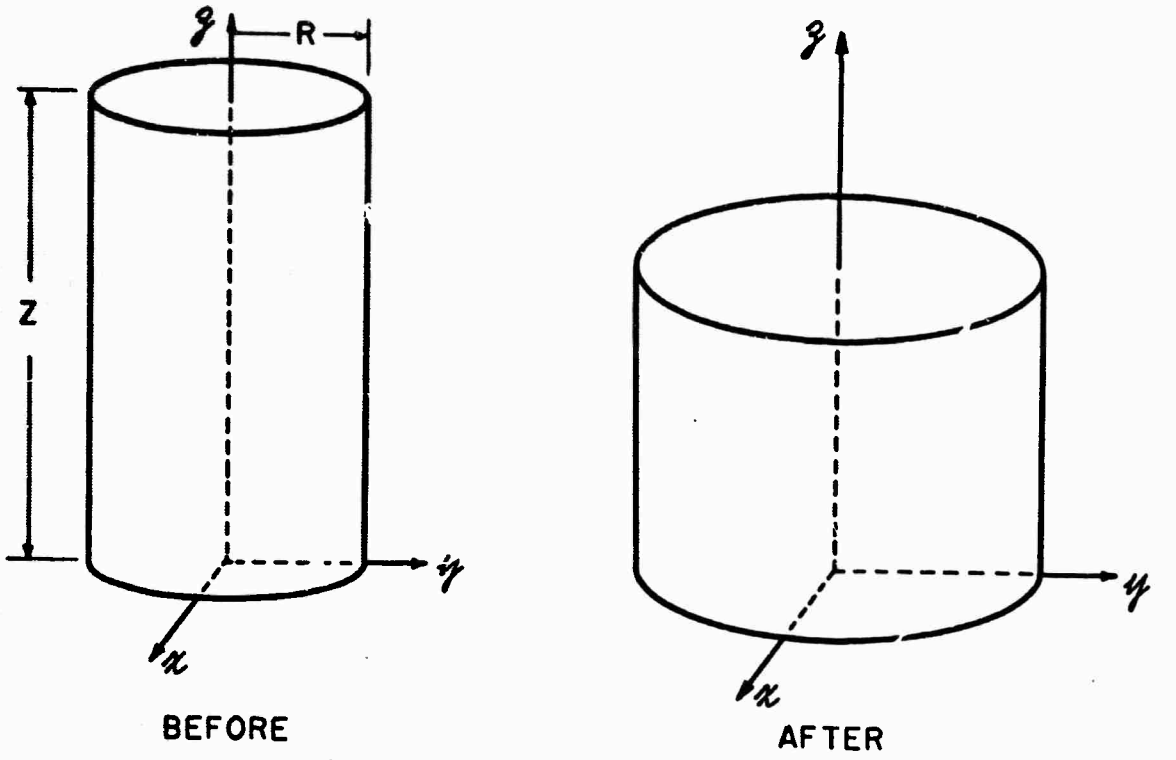


BEFORE AFTER

a.) HOMOGENEOUS DEFORMATION

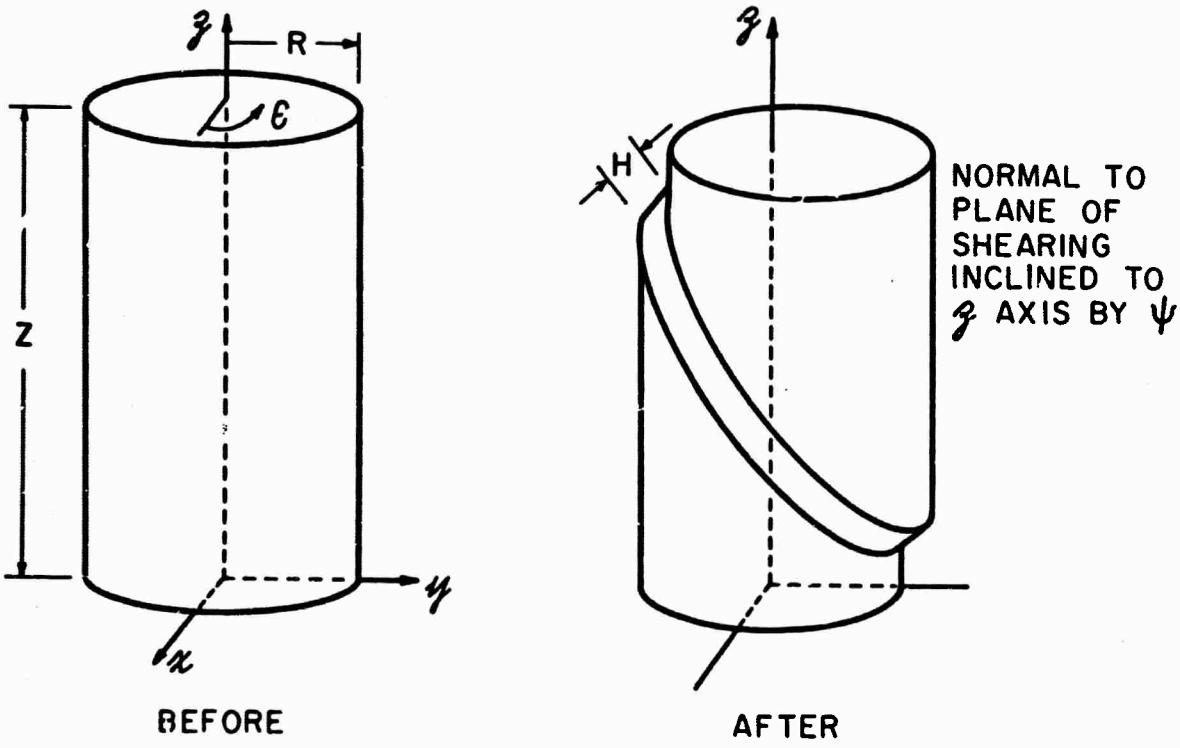


BEFORE AFTER

b.) SHEARING DEFORMATION

FIG. 1 TWO MODES OF DEFORMATION FOR THE TRIAXIAL TEST.

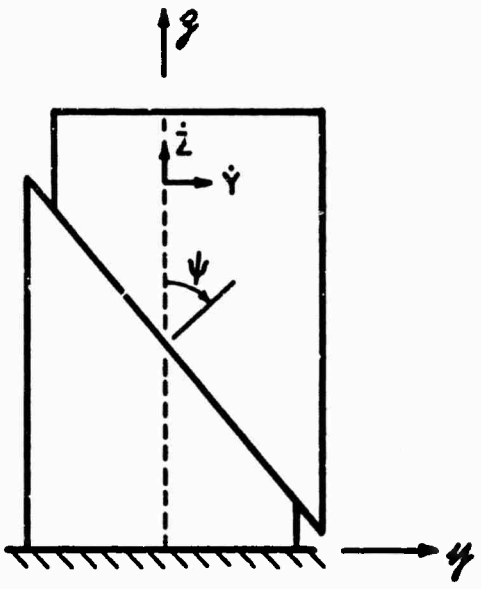


FIG. 2 MODE OF DEFORMATION FOR SHEARING MOTION WHEN THE CORRESPONDING $\dot{W} < 0$

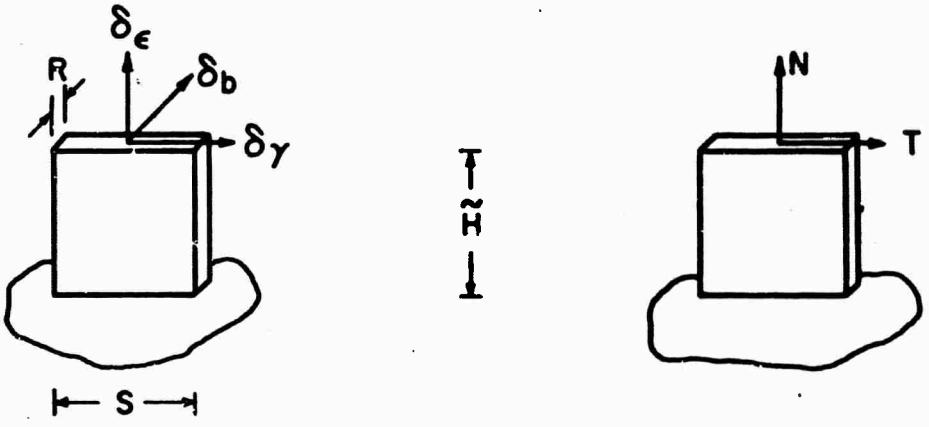


a. b.

FIG. 3 PLANE ELEMENT OF MEMBRANE SHOWING
a.) DISPLACEMENTS
b.) FORCES

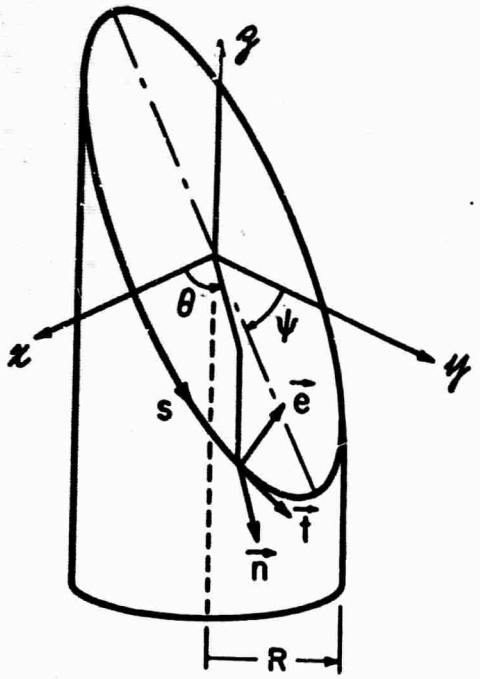


$\vec{n}$ NORMAL TO CYLINDER SURFACE

$\vec{t}$ // PLANE OF SHEARING AND $\perp \vec{n}$

$\vec{n}, \vec{t}, \vec{e}$ ARE EACH UNIT LENGTH AND MUTUALLY PERPENDICULAR

FIG. 4 SECTION OF THIN MEMBRANE BELOW SHEARING PLANE SHOWING VECTORS $\vec{n}$, $\vec{t}$, AND $\vec{e}$